Optical diode effect in the room-temperature multiferroic BiFeO₃

I. Kézsmárki,[1] U. Nagel,[2] S. Bordács,[1] R. S. Fishman,[3] J. H. Lee,[3] H. T. Yi,[4] S.-W. Cheong,[4] and T. Rõõm[2]

[1] *Department of Physics, Budapest University of Technology and Economics and MTA-BME*
Lendület Magneto-optical Spectroscopy Research Group, 1111 Budapest, Hungary
[2] *National Institute of Chemical Physics and Biophysics, 12618 Tallinn, Estonia*
[3] *Materials Science and Technology Division, Oak Ridge National Laboratory, Oak Ridge, Tennessee 37831, USA*
[4] *Rutgers Center for Emergent Materials and Department of Physics and Astronomy,*
Rutgers University, Piscataway, New Jersey 08854, USA

Multiferroics permit the magnetic control of the electric polarization and electric control of the magnetization[1–8]. These static magnetoelectric (ME) effects are of enormous interest: The ability to read and write a magnetic state current-free by an electric voltage would provide a huge technological advantage[5–8]. Dynamic or optical ME effects are equally interesting because they give rise to unidirectional light propagation as recently observed in low-temperature multiferroics[9–14]. This phenomenon, if realized at room temperature, would allow the development of optical diodes which transmit unpolarized light in one, but not in the opposite direction. Here, we report strong unidirectional transmission in the room-temperature multiferroic BiFeO₃ over the gigahertz–terahertz frequency range. Supporting theory attributes the observed unidirectional transmission to the spin-current driven dynamic ME effect. These findings are an important step toward the realization of optical diodes, supplemented by the ability to switch the transmission direction with a magnetic or electric field.

BiFeO₃ is by the far most studied compound among multiferroic and magnetoelectric materials. While experimental studies have already reported about the first realizations of the ME memory function using BiFeO₃ based devices[5–8], the origin of the ME effect is still under debate due to the complexity of the material. Because of the low symmetry of iron sites and iron-iron bonds, the magnetic ordering can induce local polarization via each of the three canonical terms[15] – the spin-current, exchange-striction and single-ion mechanisms. While the spin-current term has been identified as the leading contribution to the magnetically induced ferroelectric polarization in various studies[4,16,17], the spin-driven atomic displacements[18] and the electrically induced shift of the spin-wave (magnon) resonances[19] were interpreted based on the exchange-striction and single-ion mechanisms, respectively.

In the magnetically ordered phase below T_N=640 K, BiFeO₃ possesses an exceptionally large spin-driven polarization[18], if not the largest among all known multiferroic materials. Nevertheless, its systematic study has long been hindered by the huge lattice ferroelectric polarization ($\mathbf{P}_0$) developing along one of the cubic $\langle 111 \rangle$ directions at the Curie temperature T_C=1100 K and by

the lack of single-domain ferroelectric crystals. Owing to the coupling between $\mathbf{P}_0$ and the spin-driven polarization, in zero magnetic field they both point along the same [111] axis. A recent systematic study of the static ME effect revealed additional spin-driven polarization orthogonal to [111][17].

The optical ME effect of the magnon modes in multiferroics, which gives rise to the unidirectional transmission in the gigahertz–terahertz frequency range, has recently become a hot topic in materials science. The difference in the absorption coefficients (α) of beams counterpropagating in such ME media—called directional dichroism—can be expressed for linear light polarization as[14,20]

$$\Delta\alpha_k(\omega) = \alpha_{+k}(\omega) - \alpha_{-k}(\omega) \approx \frac{2\omega}{c}\Im\{\chi_{\gamma\delta}^{me}(\omega) - \chi_{\delta\gamma}^{em}(\omega)\}. \tag{1}$$

The dynamic ME susceptibility tensors $\hat{\chi}^{me}(\omega)$ and $\hat{\chi}^{em}(\omega)$ respectively describe the magnetization generated by the oscillating electric field of light, $\Delta M_\gamma^\omega = (\varepsilon_0/\mu_0)^{1/2}\chi_{\gamma\delta}^{me}(\omega)E_\delta^\omega$, and the electric polarization induced by its oscillating magnetic field, $\Delta P_\delta^\omega = (\varepsilon_0\mu_0)^{1/2}\chi_{\delta\gamma}^{em}(\omega)H_\gamma^\omega$. Here ε_0 and μ_0 are the vacuum permittivity and permeability, respectively, while γ and δ stand for the Cartesian coordinates. Since the two cross-coupling tensors are connected by the time-reversal operation $[\ldots]'$ according to $[\chi_{\gamma\delta}^{me}(\omega)]' = -\chi_{\delta\gamma}^{em}(\omega)$, the directional dichroism becomes $\Delta\alpha_k(\omega) = \frac{2\omega}{c}\Im\{\chi_{\gamma\delta}^{me}(\omega) - [\chi_{\gamma\delta}^{me}(\omega)]'\}$. In other words, the directional dichroism emerges for simultaneously electric- and magnetic-dipole active excitations and its magnitude is determined by the time-reversal odd parts of the off-diagonal $\chi_{\gamma\delta}^{me}(\omega)$ tensor elements[10,11,20–22]. The schematic representation of the optical diode function in ME media is shown in Fig. 1.

In the cycloidal spin state of BiFeO₃[23], several low-frequency collective modes have been observed by spectroscopic methods including light absorption[24,25] and Raman spectroscopy[6,19,26]. Though the electric-field-induced shift of the resonance frequencies observed in the Raman study indicates the ME nature of these magnon modes[19], the optical ME effect has not been investigated in BiFeO₃. Here, we performed absorption measurements in the gigahertz–terahertz spectral range on single-domain ferroelectric BiFeO₃ crystals[27] with $\mathbf{P}_0$ along [111] between room temperature and T=4 K in magnetic fields up to μ_0H=17 T. We found that some of
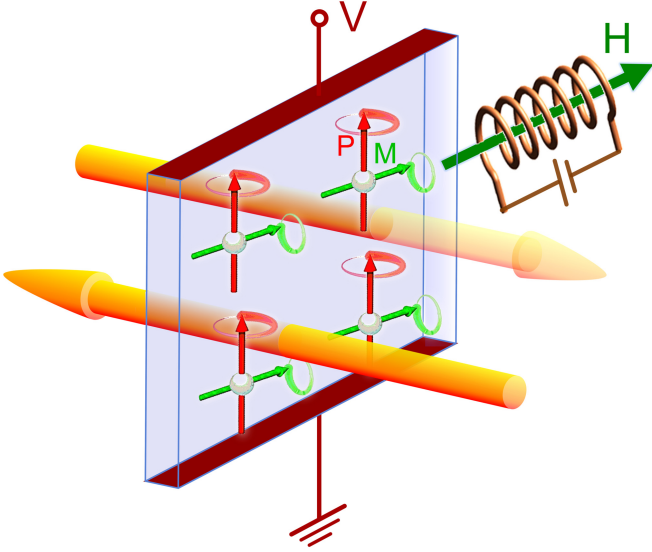
FIG. 1: | **Optical diode function in multiferroics.** Ferro-type ordering of the local electric dipoles (red arrows) and magnetic moments (green arrows) produces a ferroelectric polarization P and a spontaneous magnetization M, respectively. Light interacts with both ferroic order parameters, hence, upon illumination P and M oscillate coherently with the electromagnetic field around their equilibria. The light induced polarization has contributions from both the usual dielectric permittivity and the optical ME effect $\chi^{em}(\omega)$. While the first contribution is independent of the light propagation direction, the polarization induced via the optical ME effect has opposite sign for counter-propagating light beams. This can give rise to either a constructive or a destructive interference between the two terms. Similarly, the magnetization dynamics is governed by the interference between the magnetization induced via the magnetic permeability and the optical ME effect $\chi^{me}(\omega)$. Consequently, the transmitted intensity depends on the propagation direction (intense and pale yellow beams) even for unpolarized light and can be exploited to produce optical diodes transmitting light in one, but not in the opposite direction. The transmitting direction can be reversed by switching the sign of either P via an electric voltage (V) or M by an external magnetic field (H).

FIG. 2: | **Experimental configurations used to detect unidirectional transmission in BiFeO$_3$.** **a,** Pseudocubic unit cell of BiFeO$_3$ showing the positions of Bi, Fe and O ions. The lattice ferroelectric polarization, $\mathbf{P}_0\|[111]$, is schematically indicated on the Fe site. **b,** Illustration of the three equivalent directions of the cycloidal ordering vector $\mathbf{q}_i$ on the Fe sublattice. The frame of reference is common to all panels. **c,** In magnetic fields ($\pm H$) applied along $[1\bar{1}0]$, cycloidal domains with $\mathbf{q}_2$ and $\mathbf{q}_3$ are equally favoured, while the domain with $\mathbf{q}_1$ is suppressed[28,29]. **d,** In magnetic fields ($\pm H$) applied along $[110]$, only the cycloidal domain with $\mathbf{q}_1$ is stable[28,29]. **e** & **f,** The propagation direction ($\mathbf{k}$) and the two orthogonal polarizations of light beams traveling in the material.

the magnon modes exhibit strong unidirectional transmission. We identified the minimal set of spin-driven-polarization terms and quantitatively reproduced both the spectral shape and the field dependence of the directional dichroism solely by the spin-current mechanism.

The experimental configurations are schematically illustrated in Fig. 2. Absorption spectra were obtained for light beams propagating along $[001]$ with two orthogonal linear polarizations, $\mathbf{E}^\omega\|[1\bar{1}0]$ and $\mathbf{E}^\omega\|[110]$. Static magnetic fields ($\pm H$) were applied perpendicular to the light propagation direction along either $[110]$ or $[1\bar{1}0]$.

In simple magnets, such as ferromagnets, the sign change of the magnetization corresponds to the time reversal operation. Thus, it is equivalent to the reversal of the light propagation direction. Owing to experimental limitations, in such cases, the absorption change upon
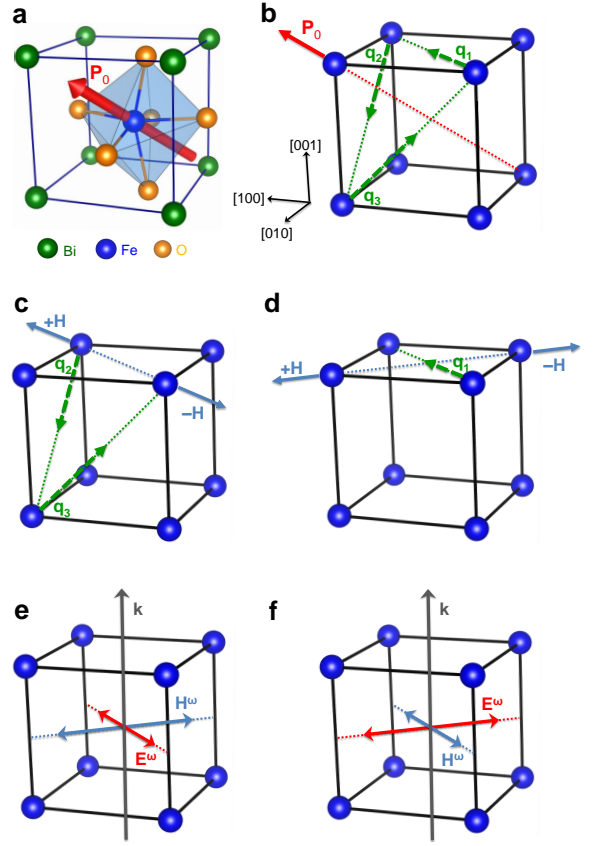
the magnetic field induced reversal of the magnetization, $\Delta\alpha_H=\alpha_{+H,+k}-\alpha_{-H,+k}$, is typically detected instead of the absorption change associated with the reversal of the light propagation direction, $\Delta\alpha_k=\alpha_{+H,+k}-\alpha_{+H,-k}$. Though the relation $\Delta\alpha_k = \Delta\alpha_H$ does not necessarily hold for complex spin structures, such as BiFeO$_3$, $\Delta\alpha_k$ and $\Delta\alpha_H$ spectra obtained from our calculations are equal within 1-2 % for the experimental configurations studied here.

Figure 3 shows the absorption spectra measured in four different configurations, i.e. for two orientations of the magnetic field and two light polarizations. The absorption coefficient at several magnon resonances depends on the sign of the magnetic field. This difference is stronger for $\mathbf{H}\|[1\bar{1}0]$ and most pronounced for the
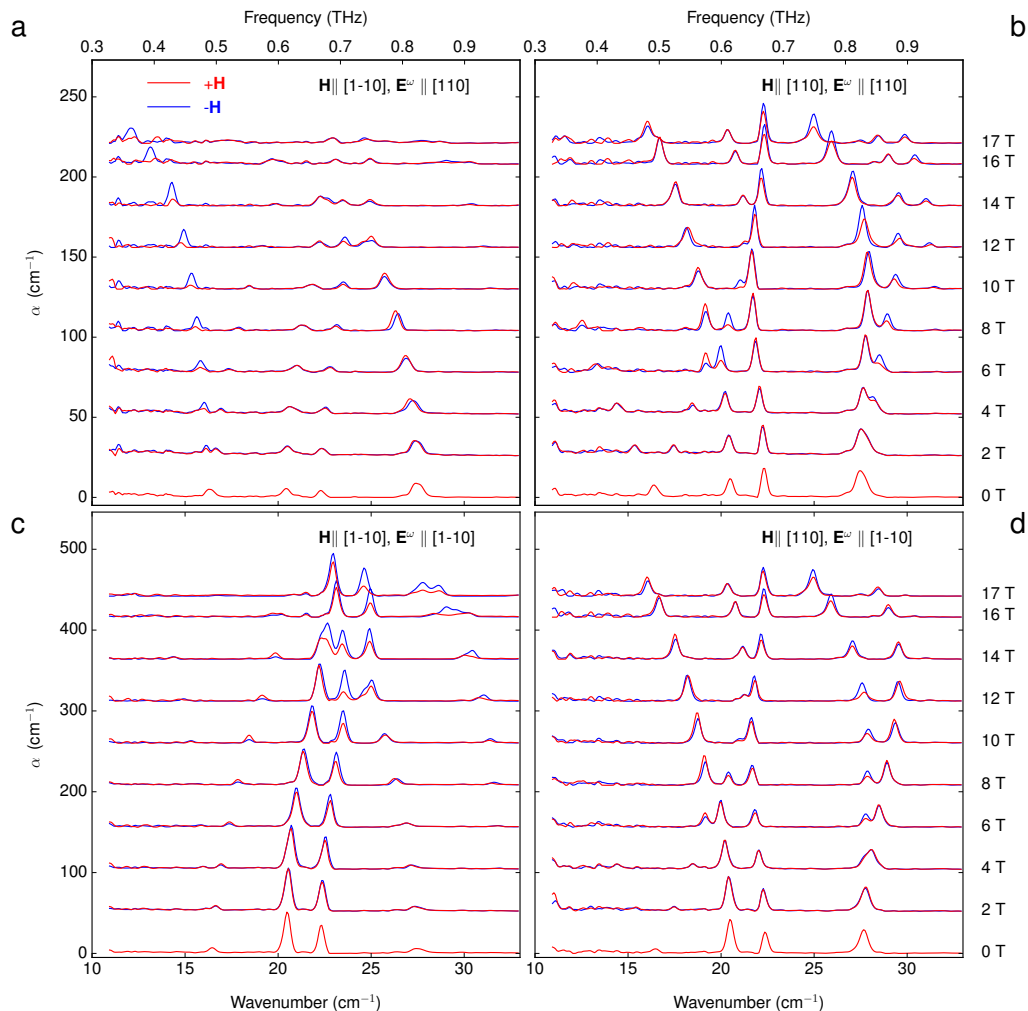
FIG. 3: | **Absorption spectra of BiFeO$_3$ in the range of magnon resonances. a-d** Magnetic field dependent part of the absorption spectra measured at T = 2.5 K in four different configurations, i.e. for the two orientations of the magnetic field (**H**) and the two orthogonal polarizations schematically shown in Fig. 2. The light propagation direction is common to all experimental configurations, **k**∥[001]. Absorption spectra measured in different magnetic fields are shifted vertically in proportion to the magnitude of the field, and spectra recorded in +H and −H are plotted with red and black lines, respectively. Spectra shown in panel **a** & **c** represent absorption form the **q**$_1$ cycloidal domain stabilized by **H**∥[1$\bar{1}$0], while spectra in panel **b** & **d** have contributions from **q**$_2$ and **q**$_3$ domains favoured by **H**∥[110].

lowest-frequency mode Ψ_0 in Fig. 3a when **H**∥[1$\bar{1}$0] and **E**$^\omega$∥[110]. With increasing magnetic field this resonance becomes almost transparent for +H, while its absorption increases for −H. We also measured the absorption spectra with both light polarizations for **H**∥[001] and could not detect any difference between ±H.

In order to reproduce the observed directional dichroism on a microscopic basis, we adopt the spin model of Refs.[28,29], which successfully describes the magnetic field dependence of the magnon resonances (see the Methods section). Similarly to the static ME effect, all the three basic mechanisms—the spin-current, exchange-striction and single-ion mechanism—can in principle contribute to the optical ME effect. By including all symmetry-allowed spin-driven polarization terms, we calculated the optical ME susceptibilities $\hat{\chi}^{me}(\omega)$ and

$\hat{\chi}^{em}(\omega)$, the dielectric permittivity $\hat{\varepsilon}(\omega)$ and the magnetic permeability $\hat{\mu}(\omega)$[14,20]. Next, we numerically solved the Maxwell equations by including these response functions in the constitutive relations and calculated the transmission of linearly polarized incoming beams for both backward and forward propagation. The same calculation was done for both field directions, ±H. As already mentioned, we found $\Delta\alpha_k \approx \Delta\alpha_H$ irrespective of the magnitude of H.

To identify the spin-driven polarization terms relevant to the optical ME effect, we performed a systematic fitting of the measured $\Delta\alpha_H(\omega)$ by treating the magnitude of the different terms as free parameters. We found that the directional dichroism spectra are closely reproduced

by the following two types of spin-current terms

$$P_\alpha^{SC} = \frac{1}{N} \sum_{\langle i,j \rangle} \{\lambda_\alpha^{(1)}[\mathbf{e}_{i,j}\times(\mathbf{S}_i\times\mathbf{S}_j)]_\alpha + (-1)^{n_i}\lambda_\alpha^{(2)}[\mathbf{S}_i\times\mathbf{S}_j]_\alpha\}$$

$$(2)$$

where the summation goes over neighbouring spins connected by unit vectors $\mathbf{e}_{i,j}$ and the integer n_i labels the hexagonal layers along [111]. The dynamic ME effect generated by the spin-current terms is described by the coupling constants $\lambda_\alpha^{(1)}$ and $\lambda_\alpha^{(2)}$, where $\alpha = x',y',z'$ stands for the three coordinates along the axes $\mathbf{x}'\|\mathbf{q}_i$, $\mathbf{y}'\|(\mathbf{P}_0\times\mathbf{q}_i)$ and $\mathbf{z}'\|\mathbf{P}_0$ (see Fig. 2b).

Figure 4 shows the comparison between the measured and calculated directional dichroism spectra for $\mathbf{H}\|[1\bar{1}0]$ with the two orthogonal light polarizations, $\mathbf{E}^\omega\|[1\bar{1}0]$ and $\mathbf{E}^\omega\|[110]$. The best fit was obtained with three independent parameters: $\lambda_{x'}^{(1)}=0$, $\lambda_{y'}^{(1)}=-2\lambda_{z'}^{(1)}\approx57.0\pm3.1\,\mathrm{nC/cm^2}$, $\lambda_{x'}^{(2)}=\lambda_{y'}^{(2)}\approx34.5\pm2.4\,\mathrm{nC/cm^2}$, $\lambda_{z'}^{(2)}\approx11.8\pm2.9\,\mathrm{nC/cm^2}$. The population of the two cycloidal domains with $\mathbf{q_2}$ and $\mathbf{q_3}$ propagation vectors was kept equal[28,29]. We note that this limited set of parameters provides only a semi-quantitative description of the mean absorption spectra, $\overline{\alpha}(\omega)=\alpha_{+H,+k}(\omega)+\alpha_{-H,+k}(\omega)$.

We found that additional terms did not further improve the quality of the fit. Hence, the optical ME effect in $BiFeO_3$ is dominated by two types of spin-current polarizations, while the exchange-striction and single-ion polarization terms do not significantly contribute to it. This stems from the general nature of the spin dynamics in $BiFeO_3$. Due to the very weak on-site anisotropy acting on the $S=5/2$ iron spins, each magnon mode corresponds to pure precessions of the spins, where the oscillating component of the spin on site i, $\delta\mathbf{S}_i^\omega$, is perpendicular to its equilibrium direction, $\mathbf{S}_i^0$. This is in contrast to the spin stretching modes observed in highly anisotropic magnets[21]. Since neighbouring spins are nearly collinear in the cycloidal state with extremely long (62 nm) pitch[23], a dynamic polarization is efficiently induced via spin-current terms such as $\delta\mathbf{P}_i^\omega \propto \mathbf{S}_i^0 \times \delta\mathbf{S}_{i+1}^\omega$. In contrast, the dynamic polarization generated by exchange-striction terms such as $\delta\mathbf{P}_i^\omega \propto \mathbf{S}_i^0 \cdot \delta\mathbf{S}_{i+1}^\omega$ is nearly zero.

Despite its success in quantitatively describing the directional dichroism spectra observed for $\mathbf{H}\|[1\bar{1}0]$, our model may not be complete. When light propagates along [001], we predict that directional dichroism should be absent for a magnetic field along $[\eta\eta\kappa]$. While this is in agreement with $\Delta\alpha_H=0$ found for $\mathbf{H}\|[001]$, it cannot account for the finite directional dichroism discerned in Figs. 3c and 3d for $\mathbf{H}\|[110]$. This discrepancy may come from additional anisotropy terms, neglected in the microscopic spin Hamiltonian adopted from Refs.[28,29], which further reduce the symmetry of the magnetic state and allow the weak directional dichroism observed for $\mathbf{H}\|[110]$.
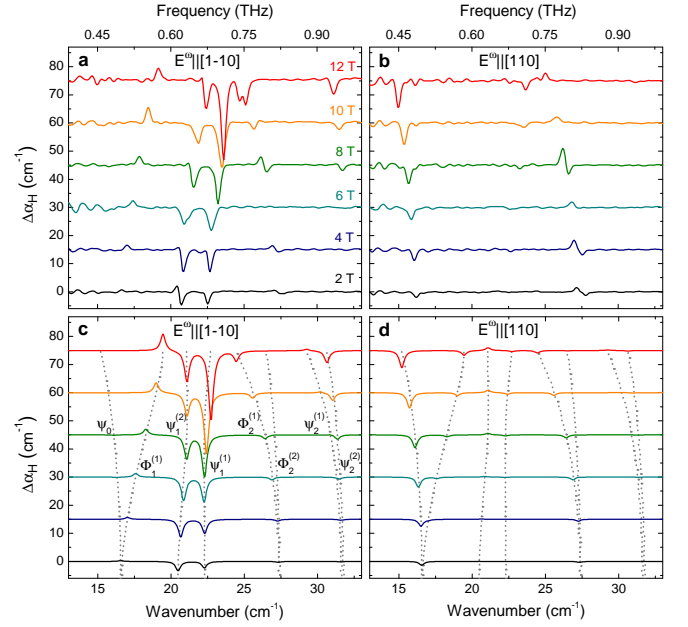
Finally, we turn to the temperature dependence of the

FIG. 4: | **Directional dichroism spectra of BiFeO₃ in the range of magnon resonances. a & b,** Magnetic field dependence of the directional dichroism spectra measured as $\Delta\alpha_H(\omega)$ at $T=2.5\,\mathrm{K}$ with the two orthogonal polarizations $\mathbf{E}^\omega\|[1\bar{1}0]$ and $\mathbf{E}^\omega\|[110]$, respectively. Spectra obtained in different magnetic fields are shifted vertically in proportion to the magnitude of the field, which was applied along $[1\bar{1}0]$. The field values (common to each panel) are indicated with labels on the top of the spectra in panel **a. c & d,** Directional dichroism spectra predicted by our model for the case of panels **a & b,** respectively. The calculated mode frequencies are indicated by dashed lines. For the assignment of the different modes see Refs.[28,29].

directional dichroism presented in Fig. 5 for $\mathbf{H}\|\mathbf{E}^\omega\|[1\bar{1}0]$. With increasing temperature the magnon modes soften[25] and both the mean absorption and the directional dichroism are reduced. Nevertheless, the modes $\Psi_1^{(1)}$ and $\Phi_2^{(1,2)}$ still exhibit considerable directional dichroism, $\Delta\alpha_H\approx5\,\mathrm{cm^{-1}}$ at room temperature. At low temperatures, almost perfect unidirectional transmission was observed for the lowest-energy mode Ψ_0 with orthogonal light polarization ($\mathbf{E}^\omega\|[110]$). Though we expect the same at room temperature, Ψ_0 is out of our limited spectral window at high temperatures.

The emergence of strong optical ME effect and the corresponding unidirectional transmission require the simultaneous breaking of the space- and time-inversion symmetries by the coexistence of ferroelectricity and (anti)ferromagnetism. While these optical ME phenomena have been investigated recently in various materials hosting multiferroicity at low temperatures, here we studied the unidirectional transmission in the spin excitation spectrum of $BiFeO_3$[5–8], the unique multiferroic compound offering a real potential for room temperature applications up to date. We found that the optical ME effect in $BiFeO_3$ is robust enough to generate con-
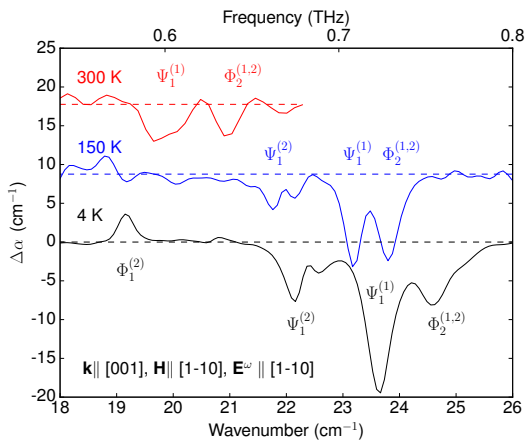
FIG. 5: | **Temperature dependence of the directional dichroism in BiFeO$_3$.** Directional dichroism spectra measured in $\mu_0 H=\pm 12\,$T at $T=$4, 150 and 300 K. The magnetic field was applied along $[1\bar{1}0]$ and $\mathbf{E}^\omega \| [1\bar{1}0]$. Modes $\Psi_1^{(1)}$ and $\Phi_2^{(1,2)}$ soften and get weaker with increasing temperature, but are still clearly observable even at 300 K. The $\Psi_1^{(2)}$ is visible until 150 K while the $\Phi_1^{(2)}$ cannot be detected reliably already at 150 K.

siderable directional dichroism in the gigahertz-terahertz range even at room temperature. Based on the current progress achieved in the electric control of the magnetization in BiFeO$_3$, we expect that the magnetic switching of the transmission direction, demonstrated here, can be complemented by the electric control of the optical ME effect. Because these functionalities exist at room temperature, they can pave the way for the development of optical diodes with electric and/or magnetic control.

Methods

Absorption measurements in the terahertz frequency range. The terahertz spectroscopy system consists of a Martin-Puplett type interferometer with a Si bolometer operating at 300 mK and a mercury lamp. At high temperatures the spectral window of the measurement was limited by the strong radiation load on the detector. The light is directed to the sample using light pipes. The sample is located in the He exchange gas filled sample chamber, which is placed into the cold bore of a 17 T superconducting solenoid.

The measurement sequence was started by applying high magnetic fields ($\geq 12\,$T) at 4 K for tens of minutes. For $\mathbf{H} \parallel [110]$ and $[1\bar{1}0]$, this procedure respectively populates a single magnetic domain with $\mathbf{q}_1$ and two domains with $\mathbf{q}_2$ and $\mathbf{q}_3$. Next, spectra were measured in different $\pm H$ fields. We did not see any change in the magnetic domain population when the $-17\,$T field was applied after $+17\,$T.

The zero field absorption spectrum was subtracted from the spectra measured in finite fields. This pro-

cedure cancels out diffraction and interference effects caused by the sample. The differential absorption coefficient $\alpha(H)-\alpha(0) = -\ln[I(H)/I(0)]d^{-1}$, where $I(0)$ and $I(H)$ are light intensity spectra in zero and H field. The lower envelope of the whole set of differential absorption spectra measured in different fields was used to calculate the zero field spectrum. Magnetic field dependent absorbtion spectra were evaluated as a sum of the zero field spectrum and the corresponding differential spectra. Note that by this method only the field-dependent part of this absorption is recovered and field-independent features are not captured. While this can cause an ambiguity of the mean absorption, the directional dichroism spectrum $\Delta\alpha_H = \alpha(+H) - \alpha(-H)$ are free of such uncertainties.

Theoretical calculations. The cycloid of BiFeO$_3$ is controlled by two Dzyaloshinskii-Moriya (DM) interactions and an easy-axis anisotropy K along the ferroelectric polarization $\mathbf{P}_0$. Whereas the DM interaction D_1 perpendicular to $\mathbf{P}_0$ is responsible for the formation of the long-period (62 nm) cycloids[30,31], the DM interaction D_2 along $\mathbf{P}_0$ is responsible for a small cycloidal tilt[31].

In a magnetic field $\mathbf{H}$, the spin state and the magnon excitations of BiFeO$_3$ were evaluated from the microscopic Hamiltonian

$$
\begin{aligned}
\mathcal{H} = & -J_1 \sum_{\langle i,j \rangle} \mathbf{S}_i \cdot \mathbf{S}_j - J_2 \sum_{\langle i,j \rangle'} \mathbf{S}_i \cdot \mathbf{S}_j \\
& + D_1 \sum_{\langle i,j \rangle} (\mathbf{z}' \times \mathbf{e}_{i,j}) \cdot (\mathbf{S}_i \times \mathbf{S}_j) \\
& + D_2 \sum_{\langle i,j \rangle} (-1)^{n_i} \mathbf{z}' \cdot (\mathbf{S}_i \times \mathbf{S}_j) \\
& - K \sum_i (\mathbf{z}' \cdot \mathbf{S}_i)^2 - 2\mu_B \mathbf{H} \cdot \sum_i \mathbf{S}_i, \quad (3)
\end{aligned}
$$

J_1 and J_2 are the nearest and the second nearest neighbour interactions, respectively. The D_1 sum, first proposed by Katsura and coworkers[16], is uniform over the lattice, while the D_2 sum alternates sign from one hexagonal layer to the next.

The nearest- and next-nearest neighbor exchange interactions $J_1=$-5.32 meV and $J_2=$-0.24 meV were obtained from recent inelastic neutron scattering measurements[32]. $D_1 \approx 0.18\,$meV is determined from the cycloidal pitch. $D_2 = 0.085\,$meV and $K=0.0051\,$meV were obtained by fitting the four magnon modes observed in zero field[24,25]. The spin state of BiFeO$_3$ is solved by using a trial spin state that contains harmonics of the fundamental ordering wavevector $\mathbf{Q}$. We then minimize the energy $\langle \mathcal{H} \rangle$ over the variational parameters of that state. A $1/S$ expansion about the classical limit is used to evaluate the magnon mode frequencies at $\mathbf{Q}$ as a function of field[28,29]. We calculated the optical ME susceptibilities, $\hat{\chi}^{me}(\omega)$ and $\hat{\chi}^{em}(\omega)$, the dielectric permittivity, $\hat{\varepsilon}(\omega)$, and the magnetic permeability, $\hat{\mu}(\omega)$, using the Kubo formula[14,20].

To determine the directional dichroism, the Maxwell

equations were numerically solved for linearly polarized monochromatic plane waves with $\pm\mathbf{k}$. Polarization rotation of the transmitted beam was found negligible. We also evaluated the directional dichroism spectra using the approximate formula in Eq. (1), which is valid when the polarization rotation of light can be neglected[14]. Eq. (1) and the numerical solution of the Maxwell equations provide nearly equivalent $\Delta\alpha_k$ spectra if parameters $\hat{\chi}^{me}(\omega)$, $\hat{\chi}^{em}(\omega)$, $\hat{\varepsilon}(\omega)$ and $\hat{\mu}(\omega)$ realistic to BiFeO$_3$ are used. Fits to the directional dichroism spectra indicate that the polarization induced by the spin current associated with D_1 and D_2 can be written in the form given by Eq.(2), where $\lambda^{(1)}$ and $\lambda^{(2)}$ are the dynamic ME couplings for the two types of terms, respectively.

Author Contributions U.N. and T.R. performed the measurements; U.N., T.R., S.B. analysed the data; S-W.C. and H.T.Y. contributed to the sample preparation; R.S.F. and J.H.L. developed the theory; I.K. wrote the manuscript; U.N., T.R. and I.K. planned the project.

---

[1] Kimura, T. *et al.* Magnetic control of ferroelectric polarization. *Nature* **426**, 55-58 (2003).

[2] Fiebig, M. Revival of the magnetoelectric effect. *J. Phys. D.: Appl. Phys.* **38**, R123-R152 (2005).

[3] W. Eerenstein, Mathur, N. D. & Scott, J. F. Multiferroic and magnetoelectric materials. *Nature* **44**, 759-765 (2006).

[4] Cheong, S.-W. & Mostovoy, M. Multiferroics: a magnetic twist for ferroelectricity. *Nat. Mater.* **6**, 13-20 (2007).

[5] Martin, L. W., Chu, Y.-H. & Ramesh R. Advances in the growth and characterization of magnetic, ferroelectric, and multiferroic oxide thin films. *Mat. Sci. Eng. R* **68**, 89-133 (2010).

[6] Sando, D. *et al.* Crafting the magnonic and spintronic response of BiFeO$_3$ films by epitaxial strain. *Nat. Mater.* **12**, 641-646 (2013).

[7] Henron, J. T. *et al.* Deterministic switching of ferromagnetism at room temperature using an electric field. *Nature* **516**, 370-373 (2014).

[8] Matsukura, F., Tokura, Y. & Ohno, H. Control of magnetism by electric fields. *Nat. Nanotechnol.* **10**, 209-220 (2015).

[9] Saito, M., Ishikawa, K., Taniguchi, K. & Arima, T. Magnetic Control of Crystal Chirality and the Existence of a Large Magneto-Optical Dichroism Effect in CuB$_2$O$_4$. *Phys. Rev. Lett.* **101**, 117402 (2008).

[10] Kezsmarki, I. *et al.* Enhanced Directional Dichroism of Terahertz Light in Resonance with Magnetic Excitations of the Multiferroic Ba$_2$CoGe$_2$O$_7$ Oxide Compound. *Phys. Rev. Lett.* **106**, 057403 (2011).

[11] Bordacs, S. *et al.* Chirality of matter shows up via spin excitations. *Nat. Phys.* **8**, 734-738 (2012).

[12] Takahashi, Y., Shimano, R., Kaneko, Y., Murakawa, H. & Tokura, Y. Magnetoelectric resonance with electromagnons in a perovskite helimagnet. *Nat. Phys.* **8**, 121-125 (2012).

[13] Takahashi, Y., Yamasaki Y. & Tokura, Y. Terahertz Magnetoelectric Resonance Enhanced by Mutual Coupling of Electromagnons. *Phys. Rev. Lett.* **111**, 037204(2013).

[14] Kezsmarki, I. *et al.* One-way Transparency of Fourcoloured Spin-wave Excitations in Multiferroic Materials. *Nat. Commun.* **5**, 3203 (2014).

[15] Jia, C., Onoda, S., Nagaosa, N. & Han, J. H. Microscopic theory of spin-polarization coupling in multiferroic transition metal oxides. *Phys. Rev. B* **76**, 144424 (2007).

[16] Katsura, H., Nagaosa, N. & Balatsky, A.V. Spin Current and Magnetoelectric Effect in Noncollinear Magnets. *Phys. Rev. Lett.* **95**, 057205 (2005).

[17] Tokunaga, M. *et al.* Magnetic control of transverse electric polarization in BiFeO$_3$. *Nat. Commun.* **6**, 5878 (2015).

[18] Lee, S. *et al.* Negative magnetostrictive magnetoelectric coupling of BiFeO$_3$. *Phys. Rev. B* **88**, 060103(R) (2013).

[19] Rovillain, P. *et al.* Electric-field control of spin waves at room temperature in multiferroic BiFeO$_3$. *Nature Materials* **9**, 975-979 (2010).

[20] Miyahara, S. & Furukawa, N. Nonreciprocal Directional Dichroism and Toroidalmagnons in Helical Magnets. *J. Phys. Soc. Jpn.* **81**, 023712 (2012).

[21] Miyahara, S. & Furukawa, N. Theory of magnetoelectric resonance in two-dimensional S = 3/2 antiferromagnet Ba$_2$CoGe$_2$O$_7$ via spin-dependent metal-ligand hybridization mechanism. *J. Phys. Soc. Jpn.* **80**, 073708 (2011).

[22] Szaller, D. *et al.* Effect of spin excitations with simultaneous magnetic- and electric-dipole character on the static magnetoelectric properties of multiferroic materials. *Phys. Rev. B* **89**, 184419 (2014).

[23] Sosnowska, I., Peterlin-Neumaier, T. and Steichle, E. Spiral magnetic ordering in bismuth ferrite. *J. Phys. C* **15**, 4835 (1982).

[24] Nagel, U. *et al.* Terahertz Spectroscopy of Spin Waves in Multiferroic BiFeO$_3$ in High Magnetic Fields. *Phys. Rev. Lett.* **110**, 257201 (2013).

[25] Talbayev, D. Long-wavelength magnetic and magnetoelectric excitations in the ferroelectric antiferromagnet BiFeO$_3$. *et al. Phys. Rev. B* **83**, 094403 (2011).

[26] Cazayous, M. *et al.* Possible Observation of Cycloidal Electromagnons in BiFeO$_3$. *Phys. Rev. Lett.* **101**, 037601 (2008).

[27] Talbayev, D., Lee, S., Cheong, S.-W. & Taylor, A. J. Terahertz wave generation via optical rectification from multiferroic BiFeO$_3$. *Appl. Phys. Lett.* **93**, 212906 (2008).

[28] Fishman, R. S., Haraldsen, J. T., Furukawa, N. & Miyahara, S. Spin state and spectroscopic modes of multiferroic

BiFeO$_3$. *Phys. Rev. B* **87**, 134416 (2013).

[29] Fishman, R. S. Field dependence of the spin state and spectroscopic modes of multiferroic BiFeO$_3$. *Phys. Rev. B* **87**, 224419 (2013).

[30] Ederer, C. & N.A. Spaldin Weak ferromagnetism and magnetoelectric coupling in bismuth ferrite. *Phys. Rev. B* **71**, 060401(R) (2005).

[31] Pyatakov, A.P. & Zvezdin, A.K. Flexomagnetoelectric interaction in multiferroics. *Eur. Phys. J. B* **71**, 419 (2009).

[32] Matsuda, M. *et al.* Magnetic Dispersion and Anisotropy in Multiferroic BiFeO$_3$. *Phys. Rev. Lett.* **109**, 067205 (2012).